

# Demonstration of Fast and Accurate Discrimination and Quantification of Chemically Similar Species Utilizing a Single Cross-Selective Chemiresistor

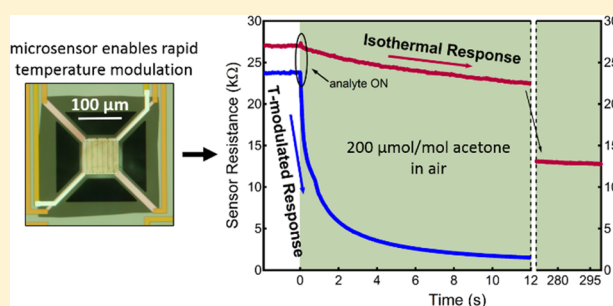
Alexander Vergara,<sup>†,‡</sup> Kurt D. Benkstein,<sup>†</sup> Christopher B. Montgomery,<sup>†</sup> and Steve Semancik<sup>\*,†</sup>

<sup>†</sup>Biomolecular Measurement Division, Material Measurement Laboratory, National Institute of Standards and Technology, Gaithersburg, Maryland 20899-8362, United States

<sup>‡</sup>Laboratory of Cellular and Synaptic Neurophysiology, National Institute of Child Health and Human Development, National Institutes of Health, Bethesda, Maryland 20892, United States

## S Supporting Information

**ABSTRACT:** Performance characteristics of gas-phase micro-sensors will determine the ultimate utility of these devices for a wide range of chemical monitoring applications. Commonly employed chemiresistor elements are quite sensitive to selected analytes, and relatively new methods have increased the selectivity to specific compounds, even in the presence of interfering species. Here, we have focused on determining whether purposefully driven temperature modulation can produce faster sensor-response characteristics, which could enable measurements for a broader range of applications involving dynamic compositional analysis. We investigated the response speed of a single chemiresistive  $\text{In}_2\text{O}_3$  microhotplate sensor to four analytes (methanol, ethanol, acetone, 2-butanone) by systematically varying the oscillating frequency (semicycle periods of 20–120 ms) of a bilevel temperature cycle applied to the sensing element. It was determined that the fastest response ( $\approx 9$  s), as indicated by a 98% signal-change metric, occurred for a period of 30 ms and that responses under such modulation were dramatically faster than for isothermal operation of the same device ( $>300$  s). Rapid modulation between 150 and 450 °C exerts kinetic control over transient processes, including adsorption, desorption, diffusion, and reaction phenomena, which are important for charge transfer occurring in transduction processes and the observed response times. We also demonstrate that the fastest operation is accompanied by excellent discrimination within a challenging 16-category recognition problem (consisting of the four analytes at four separate concentrations). This critical finding demonstrates that both speed and high discriminatory capabilities can be realized through temperature modulation.



Sensors are needed for an ever-increasing spectrum of chemical monitoring applications, ranging from environmental monitoring and process control to health screening and medical monitoring.<sup>1–4</sup> The demand is linked to developing point, network, and even “wearable” deployment scenarios where laboratory analytical instruments are inappropriate for size, cost, and operator skill requirement reasons. Development of small chemical sensors further benefits from the continued advancement of programmable electronics and low-cost communications support technology. However, the sensors must be “chemically reliable” and perform suitably in real world conditions that often involve recognizing trace-level targets in mixtures and dynamic backgrounds on an acceptable time scale. Electronic-nose (e-nose) technology, often based upon chemically induced resistance changes of the sensing elements (chemiresistors), is making some inroads toward meeting these demands for gas-phase analyses.<sup>5–7</sup> Multielement arrays can offer increased recognition capabilities in complex mixtures via the use of multiple cross-selective sensing materials (and multiple operational modes), and nanostructured materials have helped to provide higher target sensitivity within these microdevices.

There have also been advances in enhancing signal information content for better performance through the use of modulation techniques for individual chemiresistors or e-nose elements, which can include, for example, operating-temperature modulation,<sup>8–13</sup> gas-delivery modulation,<sup>14,15</sup> and analysis of the resultant transient signals.<sup>16–18</sup> Considerably less attention has been focused, however, on increasing the speed with which micro-sensors can report on the introduction, presence, and concentration of analytes within a sampled volume.<sup>19–22</sup> It is worth noting, though, that sensors based upon different operating principles can demonstrate fast responses, including, for example, oxygen sensors for automotive applications that use ionic conduction in solid electrolytes at high temperature ( $<1$  s).<sup>23</sup>

In this work, we have investigated whether purposefully driven transient phenomena based upon rapid temperature modulation

Received: April 23, 2014

Accepted: June 16, 2014

Published: June 16, 2014

can offer a route to speeding the analytical performance of a chemiresistive microsensory device. Faster recognition and quantification would enable sensors to track variations of molecular species in dynamic situations, ranging from those encountered in process control of reactors to those relevant in time-resolved breath diagnostics during respiration. While concentrating on speed, we have also explored whether our methods are suitable for maintaining an analytically informative data stream that permits good discrimination of similar compounds and varied concentration levels.

Temperature is clearly a prime factor in chemical reaction kinetics and in the interactions that occur in most chemical transduction processes, including those occurring with metal oxide semiconductors.<sup>24,25</sup> Our approach involves a simple operational mode with rapid (dwell time at each temperature step ranging from 20 to 1000 ms), two-temperature modulation of a microsensor's operating temperature to alter surface adsorbate populations and the rates of interfacial phenomena including adsorption, desorption, diffusion, and reaction. We also tune the sensor for fastest operation by systematically varying the temperature-modulation frequency. Utilizing a challenging 16-case discrimination problem, featuring four similar chemical analytes at four concentrations each, we demonstrate that our two-temperature rapid modulation approach not only reduces the response time of a single sensor element ( $<10$  s) but also, and most importantly, demonstrates high discriminatory capabilities. The frequency-optimized, bilevel scheme therefore offers both speed and accuracy and is meant to be contrasted to prior reports in which more complex sensing schemes (multipart temperature programs, varied-material arrays) were explored, primarily to find programs that would enhance selectivity.<sup>9,10,26–29</sup>

Experiments reported on here were performed using a single, microhotplate-based element populated with a thin, nano-structured  $\text{In}_2\text{O}_3$  film (Figure 1), a cross-selective sensing material known to respond with varied amplitude to different analytes.<sup>8</sup> Further information on the preparation of this type of

microsensor is given in the Supporting Information. A second, similarly prepared device was used to confirm the observed effects using a more limited data set. The analytical challenge we formulated for this work involves individual exposures to two ketones (acetone and 2-butanone) and two alcohols (ethanol and methanol), with four concentration variations (10, 50, 100 and 200  $\mu\text{mol/mol}$ ) for those gas exposures in a dry air background under dynamic conditions with a constant flow rate over the sensor (see the Supporting Information for additional experimental details). This analyte set was chosen to be chemically challenging as the sensor would need to discriminate between four volatile organic chemicals with pairs of similar chemical functionalities. Ideal sensing results would allow quick identification of both the analyte present and its concentration (one of 16 possibilities) based on sets of resistance measurements made on the  $\text{In}_2\text{O}_3$  film using interdigitated electrodes on the microhotplate platform. The basic temperature cycling program that we investigated as a transient-driver (enabled by the low thermal time constant of the microhotplate) is illustrated schematically in Figure 2. The temperatures of 450 and 150  $^{\circ}\text{C}$

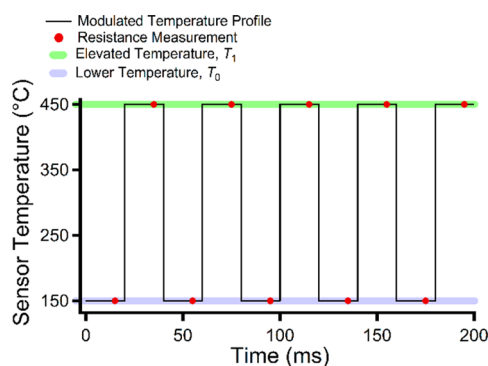


**Figure 2.** Plot displaying a 200 ms section of a pulsed-temperature program for  $p = 20$  ms used to modulate the operating temperature of the microsensor element of Figure 1a. Shaded areas of the pulsed-temperature sequence in the figure indicate the maximum (green) and minimum (lavendar) temperature levels of the modulation sequence and associated points where resistance is recorded and then utilized to generate the perturbed isotherms of Figure 3 and Figure S1 in the Supporting Information.

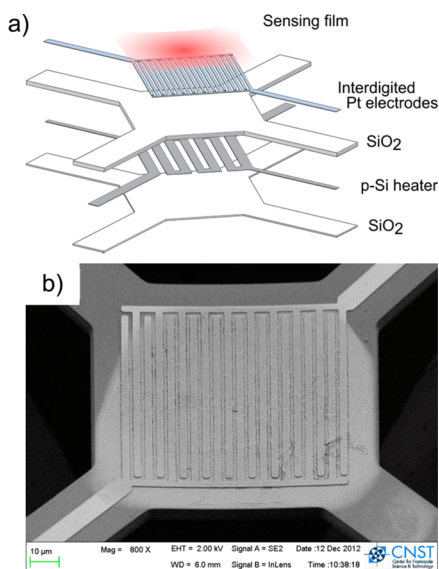


**Figure 1.** (a) Layered schematic of the low-thermal-mass micro-machined silicon platform containing the three primary components of the microsensor elements: polycrystalline silicon heater, interdigitated platinum electrodes, and metal-oxide sensing film. (b) Surface SEM view of the  $\text{In}_2\text{O}_3$  gas sensing film prepared as described in the Supporting Information.

were selected to operate the sensor within its upper and lower temperature limits, while giving a rapid and large ( $\Delta T = 300$   $^{\circ}\text{C}$ ) change in temperature between steps. Operation of the microsensor was performed for a semicycle period (dwell time at each temperature step),  $p$ , ranging from 20 to 120 ms, in 10 ms increments (as well as for  $p = 1000$  ms and  $\infty$ ) to better characterize and understand response behavior. Data were examined in sets of “perturbed isotherms”<sup>8</sup> assembled from the acquired data at both the elevated and lower temperatures of Figure 2. As stated above, our primary objective was to determine whether our cycling approach allowed faster response to a test environment for identifying a target condition.

A key observation that highlights the significant potential of our “driven” modulation approach to quicken chemiresistive analyses is shown within the panels of Figure 3 for acetone (representative response curves for the other three analytes are shown in the Supporting Information). Figure 3a,b show the perturbed isotherms, corresponding to the elevated and lower temperatures, respectively, for the sensor responding to 200  $\mu\text{mol/mol}$  of acetone with  $p = 30$  ms. Figure 3c–e shows the “true” isothermal ( $p = \infty$ ) response curves for the sensor at 450,

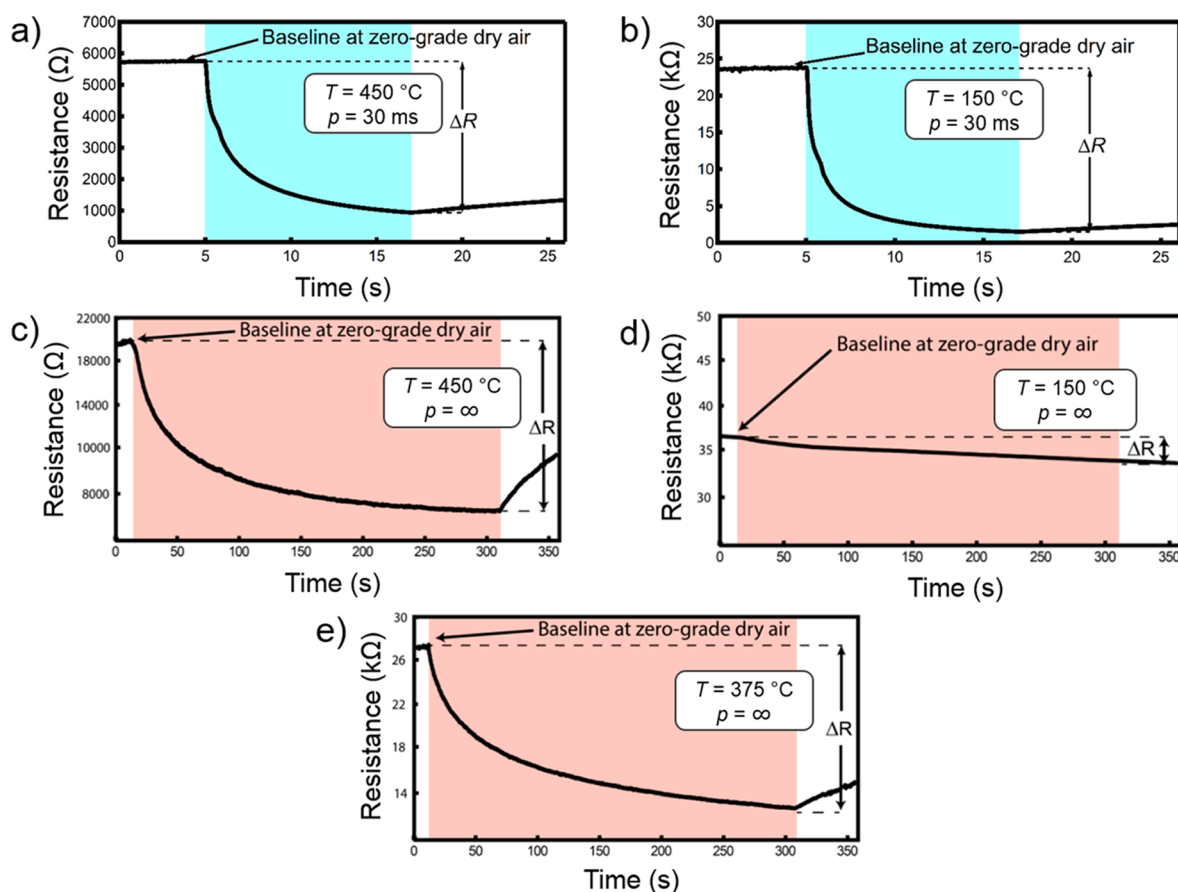


**Figure 3.** Examples of both the perturbed and the unperturbed isotherms for the microsensor responding to 200  $\mu\text{mol/mol}$  of acetone. Panels a and b show examples of the resulting perturbed isotherms corresponding to the elevated (450  $^{\circ}\text{C}$ ) and lower temperatures (150  $^{\circ}\text{C}$ ), respectively, for the sensor heating element modulated at  $p = 30$  ms. Panels c, d, and e show trace response examples for the sensor in true isothermal operation at elevated (450  $^{\circ}\text{C}$ ), lower (150  $^{\circ}\text{C}$ ), and midpoint (375  $^{\circ}\text{C}$ ) temperatures, respectively. Shaded areas of the plots indicate regions of analyte exposure, with blue indicating a 12 s dose and tan indicating a 300 s dose.

150, and 375  $^{\circ}\text{C}$ , respectively. The isothermal temperatures correspond to the elevated and lower temperatures of the pulsed-temperature program (Figure 2) and a midrange temperature between the two limits. The color bands in the plots denote the duration of analyte exposures (blue represents short exposures of 12 s and tan represents long exposures of 300 s, times required to observe essentially the full associated response). We observe that the response curves for the sensor under modulated operation appear to be much faster than any of the response curves under isothermal operating conditions. This response-differential effect holds true even for the highest temperature examined under isothermal conditions (Figure 3c), indicating that the faster responses are not due exclusively to the high sensor operating temperature but are also derived from the temperature modulation. These response curves suggest that the change in response-time behavior may be attributable to kinetically limited surface and charge-exchange processes. The sensor responses to the three other analytes show qualitatively similar effects (Figure S1, Supporting Information). To better quantify the effect, the response times,  $\tau_R$ , were mathematically calculated as the time required for the rate of change of the sensor signal to reach  $\leq 2\%$  of the maximum, with the time,  $t$ , when the sensor resistance starts to change in response to the analyte introduction set to  $t = 0$  s. Figure 4 summarizes the  $\tau_R$  numbers for the four studied analytes as a function of  $p$ . We note that for large  $p$  (1000 ms,  $\infty$ ), the sensor does not truly reach its full  $\Delta R_{\text{sensor}}$ , so we estimate the

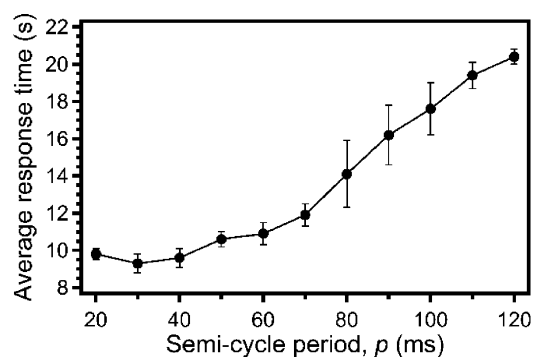


**Figure 4.** Average response times of the sensor to the four analytes as a function of the semicycle period,  $p$ . The error bars represent 1 standard deviation across the four analytes studied.

average  $\tau_R$  in those cases as  $\approx 55$  s and  $>300$  s, respectively. Thus, for  $p = 30$  ms, the average response time of the sensor for these analytes is at least a factor of 32 faster than the isothermal response time (9.3 s compared to 300 s).

These results indicate that a prime goal of the study was met, in that a simple, speed-enhancing modulation method has been identified. However, speed alone would not be acceptable if discrimination capabilities for the fast operation were greatly diminished. It may be natural to assume that slower operation might offer superior recognition, as nature often provides trade-



Table 1. Comparison of Discrimination Capabilities for  $p = 30$  ms,  $p = 1000$  ms, and  $p = \infty$  (i.e., Isothermal Operation)

$p$ (ms)	response time $\tau$ (s)	chemical species correctly predicted (%)				total accuracy
		ethanol	methanol	acetone	2-butanone	
30	9.3	95.4	96.1	92.6	100	7682/8000 96.0%
1000	$\approx 55$	98.4	90.8	95.6	100	3845/4000 96.1%
$\infty$	$>300$	88.9	93.9	48.4	47.0	2723/4000 68.1%

offs in performance characteristics. However, that assumption need not be necessarily true. Prior work has shown that the introduction of modulated operating temperatures (multiple base and excursion values) can enrich the analytical information content, particularly if one is not fixated on response speed.<sup>10,11,26,27,30</sup> In this work involving rapid two-level temperature cycling, we specifically examined the relative ability of the single microsensor to discriminate the sample cases of target exposure for the  $p$  value found to be fastest ( $p = 30$  ms). We also examined discrimination capabilities for  $p = 1000$  ms and  $p = \infty$  (i.e., isothermal operation, a common mode that commercial sensors and many sensor researchers utilize). In all cases, the data from the elevated-temperature response curves were used for analysis. The discriminatory capabilities of the sensor responses were quantified by using a Support Vector Machine (SVM) classifier<sup>31</sup> on a feature-extracted data set that represents each response to an analyte exposure as an aggregate of nine features based upon the maximum amplitude change, and an exponential moving average transform of the transient portion of the response curve (see the Supporting Information for more details).<sup>32</sup>

We first examined a chemical-recognition problem where any concentration of one of the four analytes is to be correctly reported as that given analyte (Table 1). Then we investigated results for a more challenging, semiquantitative 16-class problem where the four concentrations for each of the four analytes were also to be discriminated (see confusion matrices in Tables S1–S3 in the Supporting Information, summarized here as Table 2). For

Table 2. Semi-Quantification Success Rate in a 16-Category Discrimination Problem for  $p = 30$  ms,  $p = 1000$  ms, and  $p = \infty$  (i.e., Isothermal Operation)

temperature modulating semicycle period, $p$ , (ms)	quantification (%)	response time, $\tau$ (s)
30	89.7	9.3
1000	94.6	$\approx 55$
$\infty$	53.9	$>300$

$p = 30$  ms, and a 9.3 s response time, the recognition seen in both Tables 1 and 2 is remarkably good, especially for a single microsensor. We note that isothermal operation is least desirable, as it is very slow and offers poorer discrimination, owing to the limited information content when operating at a single temperature.<sup>16–18</sup> For slow modulation at  $p = 1000$  ms, the discriminatory capabilities of the sensor are similarly good, if not better in quantification, but sensor responses are slower on average by a factor of  $\approx 5$  than for the  $p = 30$  ms modulation. The high-performance recognition is tied closely to the observation that temperature modulation takes the signal stream from highly correlated, i.e., redundant, content (for continuous isothermal operation) to much lower correlation (for modulated perturbed isotherms).

Our frequency-dependent (frequency =  $1/(2p)$  or  $\approx 17$  Hz for  $p = 30$  ms) perturbed isotherm methodology is successful and

allows for both rapid and accurate sensing. We contrast these results (two temperatures and frequency as a parameter) with prior work from our group and others.<sup>8–10,13,19,26,27</sup> In those studies, when concentrating only on selectivity, we previously used multiple elements and inherently long and rather involved (to add analytical power) pulsed-temperature programs (long operational sequences), devised with excursions to cover many temperatures from one or multiple base levels.<sup>9,26</sup> In other cases we collected extensive databases in order to design custom programs with very specific discrimination capabilities<sup>8,10</sup> or a more complicated processing approach that identified and used only certain data from the acquired database.<sup>27</sup> In other work, the temperature dwell times did not reside in the range of 10 ms as here, but rather used 0.5 s pulses in static environments<sup>13</sup> or 5–10 s steps.<sup>19</sup> We further note that other “front-end” approaches, such as capillary diffusion of a static gas or stop flow for modulating analyte delivery, have also been employed for improving the sensing capabilities of single sensors.<sup>14,15</sup> The approach here is quite distinct in how it directly taps into the kinetic phenomena of the sensing process by using a rapid bilevel modulation, variation of  $p$ , and a straightforward optimization to identify where the greatest response speed occurs. Despite the relative simplicity of the approach, both speed and excellent recognition are attained.

The effects that we observe are both scientifically interesting and practically useful. The modulation mode shown in Figure 2 drives transient adsorption/desorption/diffusion/reaction phenomena at the surface of the  $\text{In}_2\text{O}_3$  as the microdevice platform cycles quickly between short dwell times at 150 and 450 °C, and also passes quickly and repeatedly through all temperatures between these end points. In this way, the temperature modulation manipulates adsorbate populations in a way that defines the signal stream.<sup>24,25</sup> Our frequency-dependent results (Figure 4) indicate that the square-wave thermal history of the oxide produces a minimum response time for interactions and transduction centered about 30 ms dwell times. This observed minimum value is the convolution of multiple temperature-dependent time constants that are involved for these dynamic interactional processes as well as for the transduction of surface charge transfer events into measurable conductance changes across the semiconducting  $\text{In}_2\text{O}_3$  film (which may involve percolation phenomena and trap states in the oxide).<sup>33</sup> The fact that a common trend for the four analytes with changing  $p$  is observed (see Figures 3 and 4, Figure S1 in the Supporting Information) suggests that the time range for these processes is relatively similar for these volatile organic test gases. We note that temperature modulation effects on sensor response kinetics have also been suggested for sensors operating even under lower-frequency modulation schemes but not to achieve the level of time savings that we present.<sup>19,34,35</sup> Coupled electronic and spectroscopic measurements are required to delve more deeply into the mechanistic details (e.g., exploration of electronic transport effects and vacancy-defect population variations)<sup>33,36</sup> of the enhanced response speed connected to our bilevel modulation.

We believe that the present work, while involving a single film-based sensing microelement for demonstration purposes, also has implications for further efforts on transient analysis<sup>17,37</sup> and array configurations where multiple types of sensors are simultaneously operated. Application scenarios exist where faster sensor responses to analyte introduction are useful for better process control (e.g., tracking analyte introduction and consumption in chemical- or bioreactors) or for better characterization of pulsed gases (e.g., biological olfaction testing).<sup>38</sup> Expanding beyond these well-controlled scenarios, dynamic analysis situations could incorporate tools for detecting analyte introduction or even gradual onset.<sup>39</sup> It seems likely too that the cycling and frequency domain concepts may be applicable to other next-generation microsensors<sup>20</sup> and nano-sensors, such as single, self-heated nanowires,<sup>22</sup> where the inherently low thermal time constants could/may produce even greater analytical speed and discriminatory power. On the basis of pulsed-temperature cycling and the specific results reported here, we are also exploring a more general question of the trade-off between number of microarray elements and the nature and complexity of transient-driven and temperature-enriching temperature programming for their effects on the performance characteristics of e-noses.

## ■ ASSOCIATED CONTENT

### ■ Supporting Information

Additional information exists for the Letter, including descriptions of sensor fabrication procedures, measurement methods utilized in this work, and additional data, as well as the confusion matrices for the semiquantitative analysis. This material is available free of charge via the Internet at <http://pubs.acs.org>.

## ■ AUTHOR INFORMATION

### Corresponding Author

\*E-mail: [stephen.semancik@nist.gov](mailto:stephen.semancik@nist.gov). Phone: +1 301 975 2606. Fax: +1 301 975 2643.

### Notes

The authors declare no competing financial interest.

## ■ ACKNOWLEDGMENTS

This research was performed while A.V. held a National Research Council NIH-NIST Postdoctoral Associateship Award with funding provided by NIST and the Intramural Program of the National Institute for Biomedical Imaging and Bioengineering of the NIH. We also acknowledge partial funding of this work by the Office of Naval Research. We thank Dr. P. Rogers for the precursor sensing materials and programming of the sensor control/data acquisition software.

## ■ REFERENCES

- (1) Nakata, S.; Akakabe, S.; Nakasuji, M.; Yoshikawa, K. *Anal. Chem.* **1996**, *68*, 2067.
- (2) Rogers, P. H.; Benkstein, K. D.; Semancik, S. *Anal. Chem.* **2012**, *84*, 9774.
- (3) Persaud, K. C.; Travers, P. J. In *Handbook of Biosensors and Electronic Noses: Medicine, Food, and the Environment*; Kress-Rogers, E., Ed.; CRC Press: Boca Raton, FL, 1996; p 563.
- (4) Tran, V. H.; Hiang Ping, C.; Thurston, M.; Jackson, P.; Lewis, C.; Yates, D.; Bell, G.; Thomas, P. S. *IEEE Sens. J.* **2010**, *10*, 1514.
- (5) Brattoli, M.; de Gennaro, G.; de Pinto, V.; Loiotile, A. D.; Lovascio, S.; Penza, M. *Sensors* **2011**, *11*, S290.
- (6) Shih-Wen, C.; Kea-Tiong, T. *Sensors* **2013**, *13*, 14214.
- (7) Stitzel, S. E.; Aernecke, M. J.; Walt, D. R. *Annu. Rev. Biomed. Eng.* **2011**, *13*, 1.
- (8) Rogers, P. H.; Semancik, S. *Sens. Actuators, B* **2012**, *163*, 8.
- (9) Raman, B.; Meier, D. C.; Evju, J. K.; Semancik, S. *Sens. Actuators, B* **2009**, *137*, 617.
- (10) Kunt, T. A.; McAvoy, T. J.; Cavicchi, R. E.; Semancik, S. *Sens. Actuators, B* **1998**, *53*, 24.
- (11) Fort, A.; Gregorkiewicz, M.; Machetti, N.; Rocchi, S.; Serrano, B.; Tondi, L.; Olivieri, N.; Vignoli, V.; Faglia, G.; Comini, E. *Thin Solid Films* **2002**, *418*, 2.
- (12) Heilig, A.; Bârsan, N.; Weimar, U.; Schweizer-Berberich, M.; Gardner, J. W.; Göpel, W. *Sens. Actuators, B* **1997**, *43*, 45.
- (13) Hossein-Babaei, F.; Amini, A. *Sens. Actuators, B* **2012**, *166–167*, 419.
- (14) Szczurek, A.; Maciejewska, M.; Flisowska-Wiercik, B.; Bodzój, L. *Sens. Actuators, B* **2010**, *148*, 522.
- (15) Bahraminejad, B.; Basri, S.; Isa, M.; Hambli, Z. *Sensors* **2010**, *10*, S359.
- (16) Marco, S.; Gutierrez-Galvez, A. *IEEE Sens. J.* **2012**, *12*, 3189.
- (17) Gutierrez-Osuna, R.; Gutierrez-Galvez, A.; Powar, N. *Sens. Actuators, B* **2003**, *93*, 57.
- (18) Hierlemann, A.; Gutierrez-Osuna, R. *Chem. Rev.* **2008**, *108*, 563.
- (19) Ruiz, A. M.; Illa, X.; Díaz, R.; Romano-Rodríguez, A.; Morante, J. R. *Sens. Actuators, B* **2006**, *118*, 318.
- (20) Dai, Z.; Xu, L.; Duan, G.; Li, T.; Zhang, H.; Li, Y.; Wang, Y.; Wang, Y.; Cai, W. *Sci. Rep.* **2013**, *3*, 1669.
- (21) Helwig, A.; Müller, G.; Sberveglieri, G.; Faglia, G. *Sens. Actuators, B* **2007**, *126*, 174.
- (22) Prades, J. D.; Jimenez-Diaz, R.; Hernandez-Ramirez, F.; Cirera, A.; Romano-Rodríguez, A.; Morante, J. R. *Sens. Actuators, B* **2010**, *144*, 1.
- (23) Moos, R.; Izu, N.; Rettig, F.; Reiß, S.; Shin, W.; Matsubara, I. *Sensors* **2011**, *11*, 3439.
- (24) Barsan, N.; Weimar, U. *J. Electroceram.* **2002**, *7*, 143.
- (25) Semancik, S.; Cavicchi, R. E. *Acc. Chem. Res.* **1998**, *31*, 279.
- (26) Meier, D. C.; Evju, J. K.; Boger, Z.; Raman, B.; Benkstein, K. D.; Martinez, C. J.; Montgomery, C. B.; Semancik, S. *Sens. Actuators, B* **2007**, *121*, 282.
- (27) Raman, B.; Hertz, J. L.; Benkstein, K. D.; Semancik, S. *Anal. Chem.* **2008**, *80*, 8364.
- (28) Vergara, A.; Llobet, E.; Brezmes, J.; Ivanov, P.; Cané, C.; Gràcia, I.; Vilanova, X.; Correig, X. *Sens. Actuators, B* **2007**, *123*, 1002.
- (29) Kammerer, T.; Ankara, Z.; Schütze, A. In *EUROSENSOR XVII*, Guimarães, Portugal, 2003.
- (30) Lee, A. P.; Reedy, B. J. *Sens. Actuators, B* **1999**, *60*, 35.
- (31) Muezzinoglu, M. K.; Vergara, A.; Huerta, R. In *The 2010 International Joint Conference on Neural Networks (IJCNN)*, 2010; p 1.
- (32) Muezzinoglu, M. K.; Vergara, A.; Huerta, R.; Rulkov, N.; Rabinovich, M. I.; Selverston, A.; Abarbanel, H. D. I. *Sens. Actuators, B* **2009**, *137*, 507.
- (33) Ding, J. H.; McAvoy, T. J.; Cavicchi, R. E.; Semancik, S. *Sens. Actuators, B* **2001**, *77*, S97.
- (34) Ionescu, R.; Llobet, E.; Al-Khalifa, S.; Gardner, J. W.; Vilanova, X.; Brezmes, J.; Correig, X. *Sens. Actuators, B* **2003**, *95*, 203.
- (35) Vergara, A.; Calavia, R.; Vázquez, R. M.; Mozalev, A.; Abdelghani, A.; Huerta, R.; Hines, E. H.; Llobet, E. *Anal. Chem.* **2012**, *84*, 7502.
- (36) Cox, D. F.; Fryberger, T. B.; Semancik, S. *Phys. Rev. B* **1988**, *38*, 2072.
- (37) Vergara, A.; Sheen, D. A.; Benkstein, K. D.; Semancik, S. In preparation.
- (38) Brown, S. L.; Joseph, J.; Stopfer, M. *Nat. Neurosci.* **2005**, *8*, 1568.
- (39) Raman, B.; Shenoy, R.; Meier, D. C.; Benkstein, K. D.; Mungle, C.; Semancik, S. *IEEE Sens. J.* **2012**, *12*, 3238.